Dalton Transactions

PAPER

View Article Online
View Journal | View Issue

Cite this: *Dalton Trans.*, 2019, **48**, 17395

Synthesis and iron coordination properties of schizokinen and its imide derivative†

Hataichanok Chuljerm,[a,b] Yu-Lin Chen,[a] Somdet Srichairatanakool,[b] Robert C. Hider [a] and Agostino Cilibrizzi *[a]

Received 1st July 2019,
Accepted 13th November 2019

DOI: 10.1039/c9dt02731a

rsc.li/dalton

The iron(III) affinity constants for schizokinen and its imide derivative are reported for the first time. Surprisingly, schizokinen possesses a higher affinity for iron(III) than desferrioxamine B; log $K_{Fe^{III}}$ (FeL), 36.2 and 30.6, respectively. This increase in value is associated with the substitution of one hydroxamate function by an α-hydroxycarboxylate grouping. By virtue of the similarity of siderophore–iron(III) complexes and siderophore–gallium(III) complexes, schizokinen (which is a Gram positive siderophore) has potential for ^{68}Ga PET-based imaging.

Introduction

Siderophores, are low-molecular-weight compounds (500–1500 Da) which possess a high affinity for iron(III) ($K_f > 10^{30}$). They are secreted by bacteria, fungi and graminaceous plants for scavenging iron from the environment.[1] The majority bind iron(III) in a hexadentate fashion and the most common ligands are hydroxamate and catechol. However there is an increasing number of siderophores that have been identified that use a mixture of hydroxamate and α-hydroxycarboxylate ligands in order to bind iron(III) (Fig. 1), for instance, schizokinen (**1**),[2] aerobactin (**2**),[3] acinetoferrin (**3**),[4] nannochelin A (**4**),[5] arthrobactin (**5**),[6] rhizobactin (**6**),[7] ochrobactin A (**7**)[8] and snyechobactin A (**8**).[9] In addition to these 8 siderophores, there are many siderophore families that also utilise the same ligand composition, for instance, the ornibactins,[10] the aquachelins,[11] the loihichelins[12] and the sodachelins.[13] The advantages of forming an iron(III) complex with mixed ligands is unclear, indeed there have been no affinity constant measurements made on such compounds, in contrast to the tri-hydroxyamide and tri-catecholate siderophores.[1] For this reason it was decided to determine the affinity constant of both schizokinen (**1**) and its imide derivative (**9**) which lacks the α-hydroxycarboxylate function. Both compounds are produced by *Bacillus megaterium*.[14]

Siderophores bind gallium(III) in a similar fashion to that of iron(III)[15–17] and ^{68}Ga-siderophore complexes have been investigated for their potential to detect infections in a range of clinical circumstances.[18–20] However, most of the siderophores so far investigated for this property are associated with Gram-negative organisms. Schizokinen (**1**) is produced by *Bacillus megaterium*, a Gram-positive organism, and thus has potential for the imaging of Gram-positive organisms in the clinical situation. A knowledge of the affinity constant of schizokinen for iron(III) will provide strong indications of the affinity constant for gallium(III).[1]

Results and discussion

Synthesis of the schizokinen (1) and its cyclic imide derivative (9)

The synthesis of schizokinen (**1**)[21–23] (as well as the closely related acinetoferrin (**3**))[23,24] has been previously reported. In this work, we have adopted the procedure reported by Fadeev *et al.* (Scheme 1) with several modifications.[23] The full synthetic design is based on a di-orthogonal strategy using *tert*-butyl and benzoyloxy protections on the carboxylic and amino groups, respectively. This approach allowed us to determine the most appropriate de-protection order to obtain the two chelators **1** and **9**. The starting materials **13** and **14** were synthesised through methods reported by Guo *et al.* (for **13**)[22] and Wang and Phanstiel (for **14**).[24]

A key feature of the synthesis adopted in this investigation is the coupling of 3-*tert*-butyl citrate **13** with 1-*N*-benzoyloxy-1,3-diaminopropane **14** (Scheme 1) under microwave irradiation (40 °C for 30 min), in order to limit the generation of by-products due to degradation and side reactions.

[a]*Institute of Pharmaceutical Science, King's College London, London, SE1 9NH, UK. E-mail: agostino.cilibrizzi@kcl.ac.uk*
[b]*Department of Biochemistry, Faculty of Medicine, Chiang Mai University, Chiang Mai, 50200, Thailand*

†Electronic supplementary information (ESI) available. See DOI: 10.1039/c9dt02731a

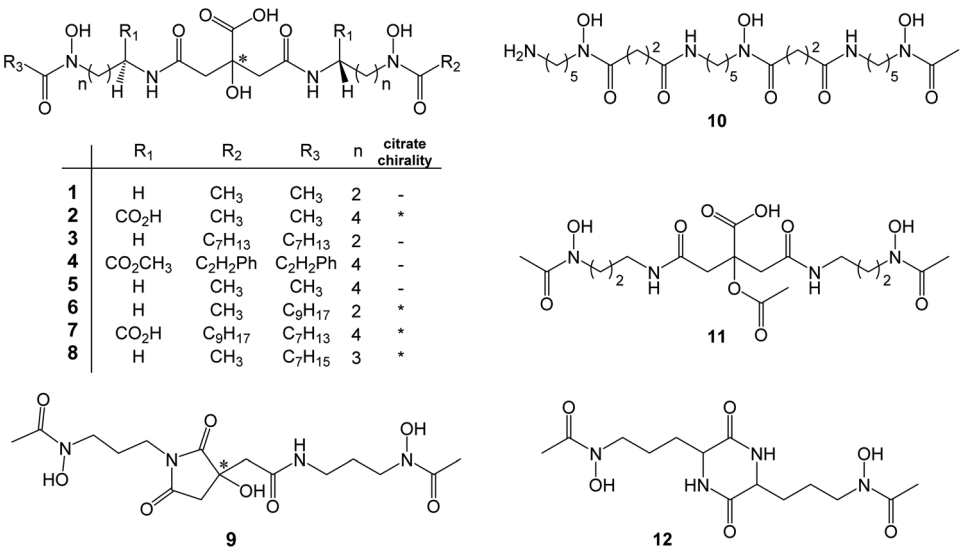

	R_1	R_2	R_3	n	citrate chirality
1	H	CH_3	CH_3	2	-
2	CO_2H	CH_3	CH_3	4	*
3	H	C_7H_{13}	C_7H_{13}	2	-
4	CO_2CH_3	C_2H_2Ph	C_2H_2Ph	4	-
5	H	CH_3	CH_3	4	-
6	H	CH_3	C_9H_{17}	2	*
7	CO_2H	C_9H_{17}	C_7H_{13}	4	*
8	H	CH_3	C_7H_{15}	3	*

Fig. 1 Chemical structures of schizokinen (**1**), α-hydroxycarboxylate siderophore analogues (**2–8**), the imide derivative of schizokinen (**9**), desferrioxamine B (**10**), acetylschizokinen (**11**) and rhodotrulic acid (**12**). The chirality of the central citrate carbon atom has not been established for siderophores **2**, **6–8** and **9**.

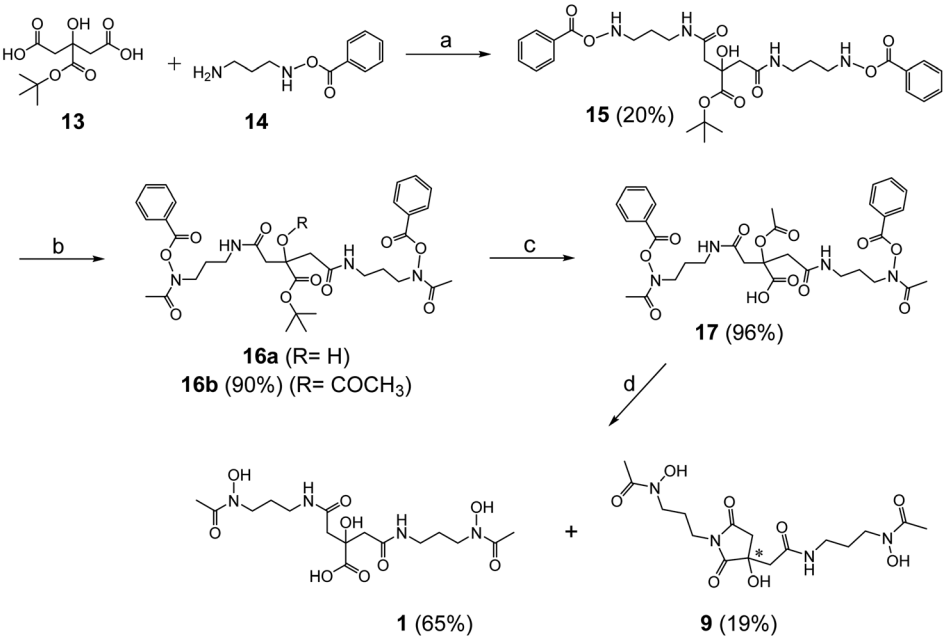

Scheme 1 Di-orthogonal approach for the synthesis of schizokinen (**1**) and its cyclic imide derivative (**9**). Reagents and conditions: (a) HATU, DIPEA, anhydrous DMF, microwave, 150 watts, 30 min, 40 °C; (b) acetyl chloride, anhydrous CH_2Cl_2, 3 h, reflux; (c) TFA/water 95 : 5, 2 h, rt; (d) 7 N NaOH, 30 min, rt.

Intermediate **15** was obtained in 20% yield. In our hands, when reacted with acetyl chloride, the major product resulting from the acetylation reaction was the tri-acetyl compound **16b**. The diacetyl compound **16a** (with the acetyl groups located on the nitrogen of the hydroxamic functions) was previously reported to be the main product.[23] Under the conditions adopted in this study, only traces (by both TLC and LC-MS) of the diacetyl derivative **16a** were detected. Column chromatography was performed to isolate pure **16b** in good yield (92%). *tert*-Butyl removal was carried out under standard conditions (TFA/water, 95 : 5). Intermediate **17** was subsequently reacted with 7 N NaOH to unmask the hydroxamic acid functions and simultaneously hydrolyse the acetyl ester on the citrate moiety, yielding a mixture of schizokinen (**1**) and its cyclic imide

derivative (**9**) in racemic form (as indicated by NMR peaks, see spectral data in section 6 of ESI†), which generates due to spontaneous dehydration reaction of **1**.[25] After removal of the hydroxamate protection groups, all glassware used to handle the free chelators was pre-treated with concentrated HCl, to prevent possible metal contamination,[26] and reversed-phase HPLC was performed to purify the final compounds. The formulation and purity of siderophores **1** and racemate **9** was confirmed by NMR and mass spectrometry (see Experimental section and sections 5 and 6 in ESI† for spectral data).

Determination of the iron(III) affinity constants for schizokinen (1) and its cyclic imide derivative (9)

The pK_a values for the hydroxamate and carboxylic functions were determined by spectrophotometric titration; the intrinsic value being reported for the two hydroxamate functions (Table 1). The pK_a value of the hydroxyl function was an estimated value, based on a previous study of citrate, malate and lactate by ^{13}C NMR.[27] No pK_a value was detected between pH 10 and pH 12.5. The composition (iron : ligand) of the two iron (III) complexes was determined by Job's plots at pH = 10.0, being 1 : 1 for schizokinen (**1**) and 2 : 3 for the schizokinen cyclic imide derivative (**9**) (Fig. 2).

Schizokinen (**1**) was found to be stable at room temperature (pH = 7.4) for a period of a week (Fig. 3a). Under the same conditions, schizokinen imide (**9**) was slowly converted to the parent schizokinen, over this same time period (Fig. 3b). When the samples were stored at −20 °C, **1** demonstrated good levels of stability (Fig. 3c and d), but **9** was slowly converted to **1** (Fig. 3d). Both the compounds were found to be sufficiently stable for titration studies. We have evaluated the half-life ($t_{1/2}$) for the hydrolysis of schizokinen imide (**9**) at pH 7.4 and room temperature as 4.4 days (see section 8 in ESI†).

Spectrophotometric titration of schizokinen (**1**) in the presence of iron yielded an isosbestic point and, after curve fitting, a log $K_{Fe^{III}}$ value of 36.2 (FeL) was determined (Table 1). Titration of schizokinen imide (**9**) in the presence of iron yielded a log affinity constant of 73.5 (Fe_2L_3). These two constants corresponded to the pFe^{III} values ($[Fe]_{total}$ = 1 μM; $[L]_{total}$ = 10 μM; pH = 7.4) of 26.8 for schizokinen and 27.8 for schizokinen imide (Table 1). These values compare favourably with corresponding pFe^{III} value for desferrioxamine (**10**), namely 25.[1]

Schizokinen (**1**) binds iron(III) at pH 7.4 almost two orders of magnitude higher than desferrioxamine B (**10**) (Table 1). This difference is clearly associated with the substitution of one hydroxamate function in desferrioxamine B by an α-hydroxycarboxylate group in schizokinen. The speciation plots of the two siderophores in the presence of iron(III) are presented in Fig. 4. There is a marked difference in their appearance over the pH range 2–5. Whereas the hydroxide anion is able to compete with desferrioxamine B for iron(III) under acid conditions, this is not the situation with schizokinen, which dominates the competition with hydroxide over the acidic pH range.

The imide derivative of schizokinen (**9**) behaves like acetylschizokinen (**11**) in its mode of iron(III) coordination.[29] The acetylation of the hydroxy function removes the avid bidentate α-hydroxycarboxylate function and, consequently, like **11**, schizokinen imide binds iron(III) as a 2 : 3 complex, as confirmed by the Job's plot (Fig. 2). The pFe^{3+} value for **9** (*i.e.* 27.8) is much higher than that of the dihydroxamate **12**, namely 21.6.[30]

The limiting factor for schizokinen imide is its susceptibility toward hydrolysis in aqueous solution at ambient temperatures. In contrast, schizokinen, is stable in aqueous solution at pH 7.0 and possesses the relatively low molecular weight of 420, it is predicted to be orally active and therefore possesses the potential to be an orally active iron chelator suitable for the treatment of systemic iron overload.[31] Furthermore, its ability to bind iron(III) more tightly than desferrioxamine B suggests that it will also bind gallium(III) with high affinity, in similar fashion to desferrioxamine.[32] Indeed, the gallium–schizokinen complex has been studied by ^{1}H NMR[17] and confirmed to be an octahedral complex involving the 6 oxygen atoms associated with the two hydroxamate groups and the α-hydroxycarboxylate function. As there is a close linear relationship between the affinity constants of Ga(III) and Fe(III) for a wide range of ligands,[15] the pGa value for schizokinen is predicted to be close to 27, rendering schizokinen with potential for ^{68}Ga PET-based imaging.

Table 1 Comparison of pK_a, log $K_{Fe^{III}}$ and pFe^{III} values between schizokinen, schizokinen imide and desferrioxamine B

	Schizokinen (**1**)	Schizokinen imide (**9**)	Desferrioxamine B (**10**)[c]
pK_a (hydroxyl)[a]	14.5	—	—
pK_a (hydroxamate)[b]	9.0	8.9	9.0
pK_a (carboxylate)	4.1	—	—
log $K_{Fe^{III}}$ (FeL)	36.2	—	30.6
log $K_{Fe^{III}}$ (Fe_2L_3)	—	73.5	—
pFe^{III} [d]	26.8	27.8	25

[a] Estimated value. [b] Intrinsic value. [c] These measurements were made in the present study. [d] $[Fe]_{total}$ = 1 μM, $[L]_{total}$ = 10 μM, pH = 7.4.

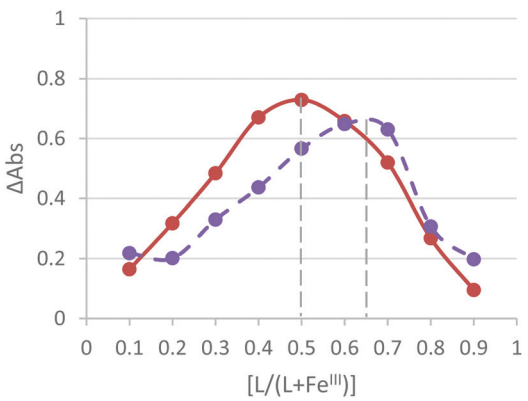

Fig. 2 Job's plots for the determination of the stoichiometry of schizokinen (**1**) (red line) and cyclic imide derivative (**9**) (*i.e.* dehydrated schizokinen; purple dashed line) with iron(III).

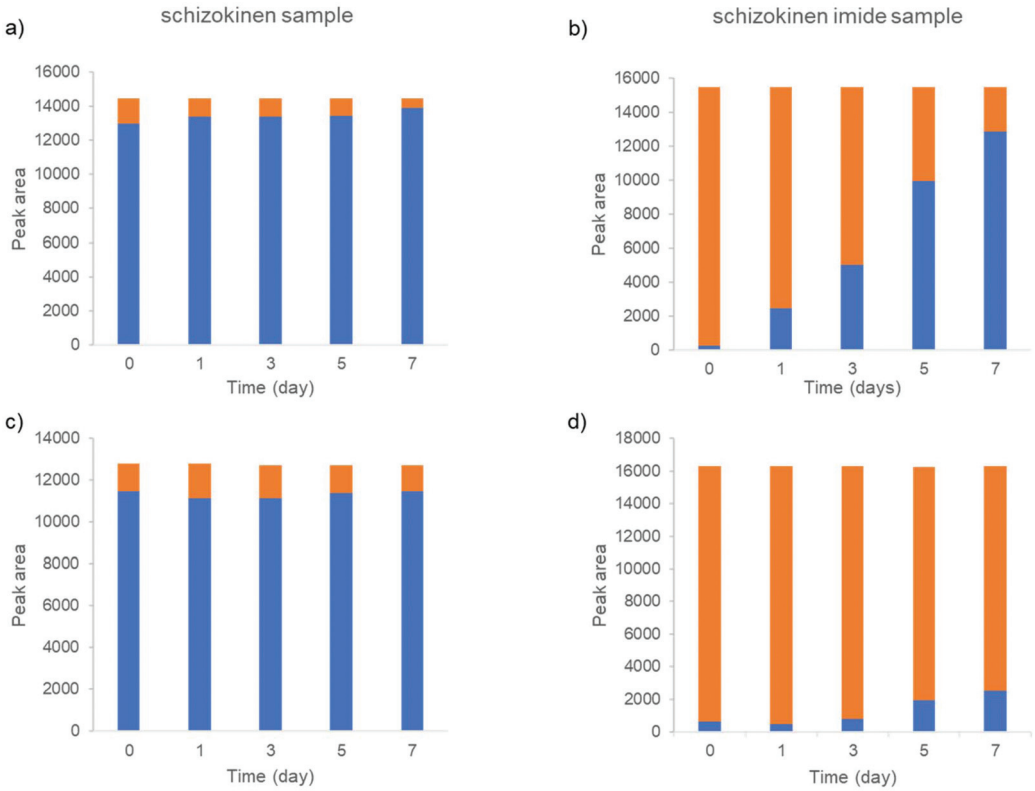

Fig. 3 Stability analysis of schizokinen (blue) and dehydrated schizokinen (*i.e.* cyclic imide) (orange) at pH = 7.4: schizokinen (a) and schizokinen imide (b) samples at room temperature for 7 days; schizokinen (c) and schizokinen imide (d) samples stored at −20 °C and thawed daily for 7 days (for UV spectra, see section 7 in ESI†).

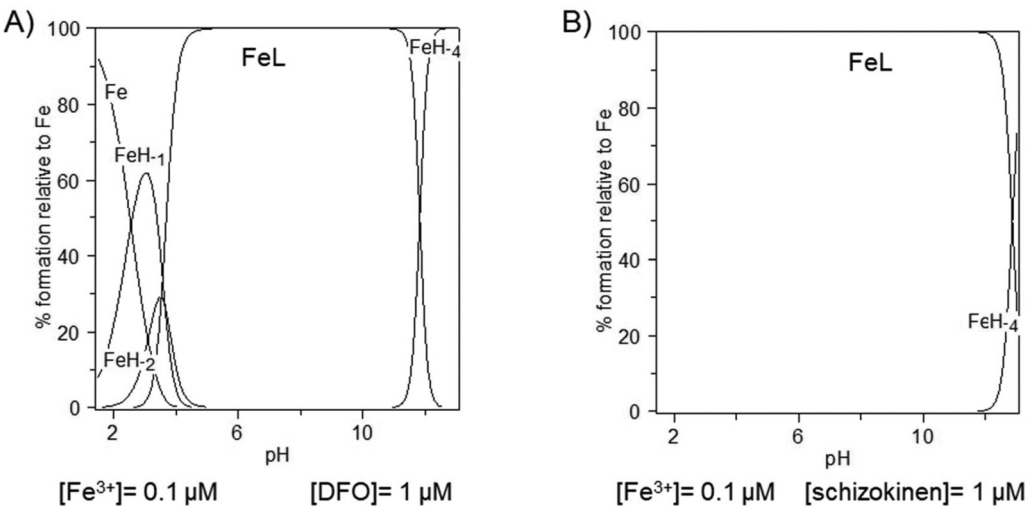

Fig. 4 Speciation plots. (A) Desferrioxamine B (10 μM), iron(III) (1 μM) and (B) schizokinen (10 μM), iron(III) (1 μM). Iron(III) hydrolysis constants were taken from Baes and Mesmer.[28]

Conclusion

A multi-step synthesis involving microwave and batch reactions has been refined and implemented to prepare the siderophore schizokinen (**1**) and its cyclic imide derivative (**9**). A synthetic approach was developed where benzoyloxy and *tert*-butyl protecting groups were integrated into a di-orthogonal protecting strategy, which proceeded smoothly, leading to good yields of all the intermediates. The overall mild conditions adopted suggest that this procedure could be useful in the general syn-

thesis of complex α-hydroxycarboxylate-based siderophores and related analogues, associated with citric acid functionalization. The affinity constant data for iron(III) indicates that schizokinen (**1**) has considerable potential as a selective iron(III) chelating agent, with potential as an orally active chelator[31] and as a suitable moiety for antibiotic therapy.[21] Schizokinen also has potential for positron–emission tomography (PET) imaging with ^{68}Ga.

The introduction of the α-hydroxycarboxylic function into the structure enhances the affinity for tribasic metal cations over and above that of tri-hydroxamate siderophores. Schizokinen imide (**9**), although possessing an extremely high pFe^{3+}, is unsuitable for therapeutic application due to its tendency to hydrolyse in aqueous systems.

Experimental details

General considerations

All reagents were purchased from chemical suppliers and used without further purification, unless otherwise mentioned. Room temperature refers to ambient temperature. Yields refer to chromatographically and spectroscopically pure compounds unless otherwise stated. Where possible, reactions were monitored by thin layer chromatography (TLC) performed on commercially available glass plates pre-coated with Merck silica gel 60 F_{254} or Merck silica gel 60 RP-18 F_{254}s. Visualisation was achieved by the quenching of UV fluorescence (λ_{max} = 254/365 nm) and by staining with iodine, ninhydrin, vanillin or potassium permanganate. All flash chromatography was carried out using slurry packed Merck 9325 Keiselgel 60 or Aldrich C_{18}-reverse phase silica gel. Nomenclatures do not follow the IUPAC naming system. ^{1}H, ^{13}C and DEPT NMR spectra were recorded using an internal deuterium lock at ambient probe temperatures on a Bruker Ascend™-400 (400 MHz) instrument. Chemical shifts (δ) are quoted in ppm, to the nearest 0.01 ppm (for ^{1}H NMRs), or 0.1 ppm (for ^{13}C NMR), and are referenced to the residual non-deuterated solvent peak. Coupling constants (J) are reported in Hertz (Hz) to the nearest 0.5 Hz. Data are reported as follows: chemical shift, multiplicity, integration, assignment and coupling constant(s). Assignments were determined either on the basis of unambiguous chemical shift or coupling pattern, or by analogy to fully interpreted spectra for related compounds. Analytical HPLC-MS experiments were performed on Agilent 1100 Series coupled to a Thermo LCQ DecaXP (operating in ES^+ or ES^- mode). A Phenomenex Luna C_{18}-(2)-HST (50 × 2 mm, 2.5 μm) column was used and the mobile phase, in linear gradient, was composed of solvent A (H_2O, +0.1% formic acid +0.05 TFA) and solvent B (acetonitrile, +0.1% formic acid +0.05 TFA). The sample solutions were prepared at a concentration of 0.1–0.01 mg/1 mL. The injection volume was 10–50 μL, the flow rate was 0.3 mL min^{-1}, the column temperature was 40 °C. The values of retention time (t_R) are given in minutes. Preparative HPLC purifications were performed using a Gemini 5μ C_{18} 110A Axia column (100 mm × 30 mm, 5 micron) and $H_2O : CH_3CN$ (gradient from 98 : 2 to 5 : 95, over 45 min) as the mobile phase. The solvents were degassed and supplemented with 0.1% formic acid prior to use. The platform consisted of a Waters RP-HPLC system (Waters 2767 autosampler for sample injection and collection; Waters 2545 and 515 pumps to deliver the mobile phase to the source) coupled to a Waters Micromass ZQ mass spectrometer (with ESI in positive and negative modes) and a Waters 2996 Photodiode Array (with detection between 190–800 nm). 3-*tert*-Butyl-citrate (**13**)[16] and 1-*N*-benzoyloxy-1,3-diaminopropane dihydrochloride (**14**)[16,17] were prepared by literature procedures (for ^{1}H NMR spectra, see section 1 in ESI†).

***tert*-Butyl 4-((3-((benzoyloxy)amino)propyl)amino)-2-(2-((3-((benzoyloxy)amino)propyl)amino)-2-oxoethyl)-2-hydroxy-4-oxobutanoate (15).** 3-*tert*-Butyl-citrate **13** (0.5 g, 2.0 mmol, 1 equiv.) was dissolved in DMF (3.0 mL). HATU (1.9 g, 5.0 mmol, 2.5 equiv.) and *N*,*N*-diisopropylethylamine (1.75 mL, 10.0 mmol, 5 equiv.) were added to the solution, followed by 1-*N*-benzoyloxy-1,3-diaminopropane dihydrochloride **14** (0.98 g, 5.0 mmol, 2.5 equiv.). The reaction was carried out under microwave irradiation (150 watts, 40 °C, 30 min). The solution mixture was extracted with water three times. The organic layer was concentrated by rotary evaporation. Flash column chromatography (eluent: ethyl acetate/MeOH 95 : 5) was used to obtain 135 mg (20.0% yield) of pure **15**. NMR and LC-MS results (for spectra, see section 2 in ESI†) are in agreement with previously reported characterisation data.[17]

***tert*-Butyl 2-acetoxy-4-((3-(*N*-(benzoyloxy)acetamido)propyl)amino)-2-(2-((3-(*N*-(benzoyloxy)acetamido)propyl)amino)-2-oxoethyl)-4-oxobutanoate (16b).** Intermediate **15** (135 mg, 0.23 mmol, 1 equiv.) was dissolved in anhydrous dichloromethane (3.0 mL). The solution was heated to reflux and acetyl chloride (68 μL, 0.945 mmol, 4.2 equiv.) in 1.0 mL of anhydrous CH_2Cl_2 was added. The reaction was refluxed for 3 h. After evaporating the solvent, the crude mixture was purified by flash column chromatography (eluent: ethyl acetate/MeOH 95 : 5). Yield after purification was 90% (150 mg). ^{1}H NMR (400 MHz, $CDCl_3$): δ 8.08 (d, 4H, Ar, J = 8.4 Hz), 7.68 (t, 2H, Ar, J = 7.6 Hz), 7.52 (t, 4H, Ar, J = 7.6 Hz), 3.80–3.93 (m, 4H, CONHCH_2), 3.25–3.35 (m, 4H, $ONCH_2$), 2.94 (AB-quartet, 4H, $COCH_2$, J = 53.2 Hz, J = 13.6 Hz), 2.07 (s, 6H, 2 × $COCH_3$), 2.05 (s, 3H, $COCH_3$), 1.80–1.85 (m, 4H, $CH_2CH_2CH_2$), 1.44 (s, 9H, 3 × $OCCH_3$). ^{13}C NMR (100 MHz, $CDCl_3$) δ 134.8 (2CH), 130.2 (4CH), 129.1 (4CH), 41.3 ($2CH_2$), 38.8 (CH_3), 36.7 ($2CH_2$), 27.9 ($3CH_3$), 27.2 ($2CH_2$), 22.1 ($2CH_2$), 21.3 (CH_3), 20.4 (CH_3). LC-MS (ESI) calcd for $C_{36}H_{46}N_4O_{12}$ 726.78 (MW), found m/z 727.02 $[M + H]^+$, 749.05 $[M + Na]^+$, t_R = 12.6.

2-Acetoxy-4-((3-(*N*-(benzoyloxy)acetamido)propyl)amino)-2-(2-((3-(*N*-(benzoyloxy)acetamido) propyl)amino)-2-oxoethyl)-4-oxobutanoic acid (17). Intermediate **16b** (150 mg, 0.21 mmol) was suspended in 6 mL of TFA/water 95 : 5 (v/v) and stirred for 2 h at room temperature. After the deprotection was complete, the reaction mixture was evaporated under vacuum and purified by flash column chromatography (eluent: $CHCl_3$/EtOH 80 : 20). The yield after purification was 96%

(135 mg). ^{1}H NMR (400 MHz, $CDCl_3$ + CD_2Cl_2): δ 10.67 (exch br s, 1H, OH), 8.08 (d, 4H, Ar, J = 7.6 Hz), 7.69 (t, 2H, Ar, J = 7.6 Hz), 7.53 (t, 4H, Ar, J = 7.6 Hz), 3.89 (t, 4H, CONHCH_2, J = 6.0 Hz), 3.32–3.41 (m, 4H, ONCH_2), 3.06 (AB-quartet, 4H, COCH_2, J = 37.2 Hz, J = 14.0 Hz), 2.07 (s, 9H, 3 × CH_3), 1.85 (q, 4H, $CH_2CH_2CH_2$, J = 6.0 Hz). LC-MS (ESI) calcd for $C_{32}H_{38}N_4O_{12}$ 670.67 (MW), found m/z 671.08 $[M + H]^+$, 693.04 $[M + Na]^+$, t_R = 11.32.

2-Hydroxy-4-((3-(*N*-hydroxyacetamido)propyl)amino)-2-(2-((3-(*N*-hydroxyacetamido)propyl) amino)-2-oxoethyl)-4-oxobutanoic acid (1, shizokinen) and *N*-hydroxy-*N*-(2-(2-(3-hydroxy-1-(2-(*N*-hydroxyacetamido)ethyl)-2,5-dioxopyrrolidin-3-yl) acetamido)ethyl)acetamide (9, cyclic imide derivative). Intermediate **17** (135 mg, 0.20 mmol) was dissolved in 7 N NaOH (5 mL) in a plastic Falcon™ tube in an ice-bath and shaked for 30 minutes at room temperature. The pH of the reaction was adjusted to 7 by the addition of 7 N HCl. The course of the reaction was monitored by TLC and LC-MS analysis, which revealed the presence of schizokinen (**1**) as the main species and the cyclic imide product (**9**) as a secondary racemic product. After evaporation of the solvent by freeze-drying, preparative HPLC was used to obtain the pure compounds. Yields after purification were 65% and 19% for **1** (55 mg) and racemate **9** (15 mg), respectively. NMR and LC-MS results (for spectra, see sections 5 and 6 in ESI†) are in agreement with previously reported characterisation data.[14,23,25,33]

Job's plots

The concentrations of the two components (iron(III) and siderophore) were continuously varied, while the total concentration was kept constant. Siderophore (1.8 mM) in ammonium acetate (pH = 10.0, 20 mM) was added to Fe^{III}–NTA (1 : 2 mmolar ratio, 1.8 mM) also in ammonium acetate (pH = 10, 20 mM) in different molar ratios ranging from 1 : 9 to 9 : 1 (siderophore : iron(III)) (see Table S1 in ESI†). The solutions were allowed to stand at 20 °C for 1 h. The absorption spectra of the solutions were recorded and the absorbances at 368 nm plotted *vs.* the molar ratio of siderophore : iron(III) (Fig. 2).

Stability studies in aqueous solution

The stability of **1** and **9** was assessed by HPLC-UV on the HP 1050 Series equipment (for spectra, see section 7 in ESI†). For all the analyses, an Agilent Zorbax SB-C18 column (2.1 mm × 100 mm, 3.5 μm) was used and the mobile phase was composed of solvent A (99.9% water, 0.1% TFA) and solvent B (99.9% acetonitrile, 0.1% TFA) used in a linear gradient (time = 0 min, 100%A and 0%B; time = 20 min, 10%A and 90%B; time = 23 min, 10%A and 90%B; time = 25 min, 100%A and 0%B; total run time 31 min) at the flow rate of 0.3 mL min^{-1}. The sample solutions were prepared by dissolving pure compounds in 5 mM ammonium acetate buffer at pH = 6.0, which was then adjusted to pH = 7.4. The injection volume was 10 μL, the column temperature was 40 °C and the UV detector wavelength was fixed at 210, 214, 230, 254 and 281 nm. The stability of siderophores was investigated under room temperature storage conditions (*i.e.* samples at room temperature were monitored daily up to 7 days). Stability under freeze/thaw conditions was also monitored for 7 days (samples were stored at −20 °C and thawed daily). The half-life ($t_{1/2}$) value of the hydrolysis was calculated by plotting the percentages of peak area against incubation time (section 8 in ESI†).

Determination of affinity constants

The automated titration used for this study consists of a Metrohm 765 Dosimat autoburette, a Mettler Toledo MP230 pH meter with SENTEK pH electrode (P11), and an HP 8453 UV-visible spectrophotometer with a Hellem quartz flow cuvette, with circulation driven by a Gilson Mini-plus #3 pump (speed capability 20 mL min^{-1}). A potassium chloride electrolyte solution (0.1 M) was used to maintain the ionic strength. The temperature of the test solutions was maintained in a thermostatic jacketed titration vessel at 25 ± 0.1 °C, using a Fisherbrand Isotemp water bath. The pH electrodes were calibrated using the software GLEE[34] with data obtained by titrating a volumetric standard HCl (0.1 M) in KCl (0.1 M) with KOH (0.1 M) under an atmosphere of argon. Analytical grade reagent materials were used in the preparation of all solutions. The solution under investigation was stirred vigorously during the experiment. For pK_a determinations, a cuvette path length of 10 mm was used, while for metal stability constants determinations, a cuvette path length of 50 mm was used (experimental concentration was *ca.* 40 μM for iron complexes). All instruments were interfaced to a computer and controlled by an in-house program. The automated titration adopted the following strategy: the pH of a solution was increased in increments of 0.1 pH unit by the addition of potassium hydroxide solution (0.1 M) from the autoburette. The pH readings were judged stable if they varied by less than 0.01 pH unit after a pre-set incubation period. For pK_a determinations, an incubation period of 1.5 min was adopted; for metal stability constant determinations, an incubation period of 3 min was adopted. The cycle was repeated until the predefined end point pH value was achieved. Titration data were analysed with the HypSpec2014 program (http://www.hyperquad.co.uk/).[35,36] The fitting spectra range for iron complexes was 400–700 nm. The associated hydrolysis constants used in the analysis were collected from Martell's critical stability constants.[37] Metal affinities of compounds in this study were determined in competition with the metal hydrolysis species in a solution at a high pH (titrated up to pH 12.0). Satisfactory fitting of both the siderophore titrations with iron was achieved. Speciation plots were calculated with the HYSS program,[38] adopting the iron(III) log hydrolysis constants, FeOH (−2.563), $Fe(OH)_2$ (−6.205), $Fe(OH)_3$ (−15.1), and $Fe(OH)_4$ (−21.883), $Fe_2(OH)_2$ (−2.843).[28]

Conflicts of interest

There are no conflicts to declare.

Acknowledgements

The authors gratefully acknowledge Dr Xiaole Kong (Hangzhou Ai Yongmei Co. Ltd, Zhejiang, China) for his help with the speciation plot analyses. This work was supported by the Newton Fund 2017/2018 from British Council and the Research and Researcher for Industries (RRi) (PHD59I0029), Thailand Science Research and Innovation (TSRI).

References

1 R. C. Hider and X. Kong, *Nat. Prod. Rep.*, 2010, **27**, 637–657.
2 M. Kreutzer, H. Koge and M. Nett, *J. Am. Chem. Soc.*, 2012, **134**, 5415–5422.
3 F. Gibson and D. I. Magrath, *Biochim. Biophys. Acta*, 1969, **192**, 175–184.
4 N. Okujo, Y. Sakakibara, T. Yoshida and S. Yamamoto, *BioMetals*, 1994, **7**, 170–176.
5 B. Kunze, W. Trowitzsch-Kienast, G. Höfle and H. Reichenbach, *J. Antibiot.*, 1992, **45**, 147–150.
6 W. D. Linke, A. Crueger and H. Diekmann, *Arch. Mikrobiol.*, 1972, **85**, 44–50.
7 M. Persmark, P. Pittman, J. S. Buyer, B. Schwyn, P. R. Gill Jr. and J. B. Neilands, *J. Am. Chem. Soc.*, 1993, **115**, 3950–3956.
8 J. D. Martin, Y. Ito, V. V. Homann, M. G. Haygood and A. Butler, *J. Biol. Inorg. Chem.*, 2006, **11**, 633–641.
9 Y. Ito and A. Butler, *Limnol. Oceanogr.*, 2005, **50**, 1918–1923.
10 H. Budzikiewicz, *Prog. Chem. Org. Nat. Prod.*, 2004, **87**, 81–237.
11 S. Kishimoto, S. Nishimura and H. Kakeya, *Chem. Lett.*, 2015, **44**, 1303–1305.
12 J. S. Martinz, G. P. Zhang, P. D. Holt, H.-T. Jung, C. J. Carrano, M. G. Haygood and A. Butler, *Science*, 2000, **287**, 1245–1247.
13 V. V. Homann, M. Sandy, A. Tincu, A. Templeton, B. Tebo and A. Butler, *J. Nat. Prod.*, 2009, **72**, 884–888.
14 X. Hu and G. L. Boyer, *BioMetals*, 1995, **8**, 357–364.
15 R. C. Hider and A. D. Hall, *Prog. Med. Chem.*, 1991, **28**, 41–173.
16 E. W. Price and C. Orvig, *Chem. Soc. Rev.*, 2014, **43**, 260–290.
17 D. J. Berry, Y. Ma, J. R. Ballinger, R. Tavaré, A. Koers, K. Sunassee, T. Zhou, S. Nawaz, G. E. Mullen, R. C. Hider and P. J. Blower, *Chem. Commun.*, 2011, **47**, 7068–7070.
18 M. Petrik, C. Zhai, H. Haas and C. Decristoforo, *Clin. Transl. Imaging*, 2017, **5**, 15–27.
19 J. A. Ioppolo, D. Caldwell, O. Beiraghi, L. Llano, M. Blacker, J. F. Valliant and P. J. Berti, *Nucl. Med. Biol.*, 2017, **52**, 32–41.
20 M. Petrik, H. Haas, M. Schrettl, A. Helbok, M. Blatzer and C. Decristoforo, *Nucl. Med. Biol.*, 2012, **39**, 361–369.
21 A. Ghosh and M. J. Miller, *J. Org. Chem.*, 1993, **58**, 7652–7659.
22 H. Guo, S. A. Naser, G. Ghobrial and O. Phanstiel IV, *J. Med. Chem.*, 2002, **45**, 2056–2063.
23 E. A. Fadeev, M. Luo and J. T. Groves, *J. Am. Chem. Soc.*, 2004, **126**, 12065–12075.
24 Q. X. Wang and O. Phanstiel, *J. Org. Chem.*, 1998, **63**, 1491–1495.
25 E. P. Storey, R. Boghozian, J. L. Little, D. W. Lowman and R. Chakraborty, *BioMetals*, 2006, **19**, 637–649.
26 A. Cilibrizzi, V. Abbate, Y. L. Chen, Y. Ma, T. Zhou and R. C. Hider, *Chem. Rev.*, 2018, **118**, 7657–7701.
27 A. M. Silva, X. Kong and R. C. Hider, *BioMetals*, 2009, **22**, 771–778.
28 C. F. Baes and R. E. Mesmer, *The Hydrolysis of Cations*, Wiley, New York, 1976.
29 J. E. Plowman, T. M. Loehr, S. J. Goldman and J. Sanders-Loehr, *J. Inorg. Biochem.*, 1984, **20**, 183–197.
30 C. J. Carrano, S. R. Cooper and K. N. Raymond, *J. Am. Chem. Soc.*, 1979, **101**, 599–604.
31 Z. D. Liu and R. C. Hider, *Med. Res. Rev.*, 2002, **22**, 26–64.
32 E. Banin, A. Lozinski, K. M. Brady, E. Berenshtein, P. W. Butterfield, M. Moshe, M. Chevion, E. P. Greenberg and E. Banin, *Proc. Natl. Acad. Sci. U. S. A.*, 2008, **105**, 16761–16766.
33 M. J. Milewska, A. Chmiak and Z. Glowacki, *J. Prakt. Chem.*, 1987, **329**, 447–456.
34 P. Gans and B. O'Sullivan, *Talanta*, 2000, **51**, 33–37.
35 P. Gans, A. Sabatini and A. Vacca, *Talanta*, 1996, **43**, 1739–1753.
36 P. Gans, A. Sabatini and A. Vacca, *Ann. Chim.*, 1999, **89**, 45–49.
37 R. Smith and A. Martell, *Critical stability constants*, Plenum Press, New York, 1977–1979.
38 L. Alderighi, P. Gans, A. Ienco, D. Peters, A. Sabatini and A. Vacca, *Coord. Chem. Rev.*, 1999, **184**, 311–318.